

CYCLOTRON LINE VARIABILITY

T. Mihara¹, K. Makishima², and F. Nagase³

¹*The Institute of Physical and Chemical Research, 2-1 Hirosawa, Wako, Saitama 351-01, Japan*

²*Dept. of Physics, School of Science, Univ. of Tokyo, 7-3-1 Hongo, Bunkyo-ku, Tokyo 113, Japan*

³*Inst. of Space and Astronautical Science, 3-1-1 Yoshinodai, Sagamihara, Kanagawa 229, Japan*

ABSTRACT

We systematically analyzed the spectra of X-ray binary pulsars observed with *GINGA* (Mihara 1995). A new model NPEX (Negative and Positive power-laws EXponential) was introduced to represent the pulsar continuum. Combining the NPEX continuum with the CYAB factor (cyclotron resonance scattering model), we successfully fit the whole-band spectra of all the pulsars. A possible physical meaning of the NPEX model is the Comptonized spectra.

By using the smooth and concave NPEX model, the cyclotron structures were detected from 12 pulsars, about a half of the 23 sources, including new discoveries from LMC X-4 and GS 1843+00. The magnetic fields were scattered in the range of $3 \times 10^{11} - 5 \times 10^{12}$ G. The distribution was shown for the first time, which is remarkably similar to that of radio pulsars with a peak at 2×10^{12} G.

The double harmonic cyclotron structures of 4U 0115+63 in 1990 changed to a single structure in 1991. The resonance energy also increased by 40 % as the luminosity decreased to 1/6. If we attribute this change to the height of the scattering region in a dipole magnetic field, the height change is ~ 1.1 km. Such changes of the resonance energies with luminosities are observed from 5 pulsars and can be explained by the accretion column height model.

INTRODUCTION

The X-ray binary pulsar is a neutron star in a contact binary system with mostly a high-mass star. The neutron star is highly magnetized ($\sim 10^{12}$ G), collimates the accreting matter onto magnetic poles and shows X-ray pulses with the rotation. The electron cyclotron resonance structure in the X-ray spectrum is the only direct method to measure the magnetic fields on the neutron star. The resonance energy is $E_a[\text{keV}] = 11.6B[10^{12}\text{G}]$. The first report of the structure was from Her X-1 (Trümper *et al.* 1978), followed by that from 4U 0115+63 by Wheaton *et al.* (1979). But for the other pulsars, the magnetic fields are estimated by a rather uncertain method using accretion spin up/down theory. Spectra of X-ray binary pulsars look non-thermal and are not explained well. Theories have been proposed (eg. Meszaros 1992), but comparison with the data has not been done much.

GINGA LAC (Turner *et al.* 1989) not only discovered cyclotron structures from many pulsars, but also enabled us to discuss on the continuum spectra. Those two are related with each other. A good representation of the continuum spectra is essential to a precise analysis of the cyclotron structure. *GINGA* observed 23 pulsars including 1 pulsar-candidate with good statistics in its 4 years and 9 months life. First we introduce a new empirical continuum model NPEX, and discuss the meaning. Next we show the magnetic fields distribution. Last we discuss the variability of the cyclotron structure.

NPEX MODEL

It is known that a typical spectrum of a binary X-ray pulsar is a power-law (POWL) below ~ 20 keV and falls off exponentially at higher energies. The reason of the exponential cutoff (ECUT) was not known. *GINGA* found cyclotron structures at the bottom of the fall-off, which lead to a physical idea that the ECUT is created by the cyclotron resonances of the fundamental, 2nd, 3rd,... harmonics. Thus early studies of pulsars with *GINGA* were done by employing a power-law (POWL) model as a continuum and a cyclotron feature as an absorption (CYAB) (Makishima and Mihara 1992). They employed two resonance, the fundamental and the 2nd harmonics, because those two are within the *GINGA* energy range. This model succeeded to explain the overall spectrum in 8–60 keV of Her X-1 (Mihara *et al.* 1990). It favored an absorption at 34 keV rather than an emission at 50keV which was uncertain in the previous observations.

$$CYAB(E) = e^{-\tau_1}, \quad \tau_1 = \frac{D_1(\frac{W}{E_a}E)^2}{(E - E_a)^2 + W^2}, \quad \tau_2 = \frac{D_2(\frac{2W}{2E_a}E)^2}{(E - 2E_a)^2 + (2W)^2},$$

Here τ_1 is optical depth of the fundamental cyclotron scattering in a classical cold plasma. τ_2 is that for the 2nd harmonic. E_a is the resonance energy, W is the width of the resonance, and D_1 and D_2 are the depths of the resonances. Resonance energy and the width of the 2nd harmonic were fixed to the double of those of the fundamental in the fitting, because the 2nd resonance was almost at the end of the energy range and it was difficult to be obtained independently.

The flux of POWL \times double CYAB's model goes back to the POWL level far above the resonance. Later the *HEAO-1* A4 spectrum of Her X-1 in 13–180 keV was published by Soong *et al.* (1990), but the data does not show the flux return. Putting the 3rd, 4th and 5th harmonics can reduce the flux, but it is not favorable because it requires larger cross section of the 3rd than the 2nd, larger the 4th than the 3rd. It is possible that optical depth of the 2nd is apparently larger than that of the fundamental because the two-photon decay of the 2nd harmonic may fill up the fundamental, but for higher harmonics than the 2nd, the reverse of the optical depths would not happen.

Another problem is on 4U0115+63, which is the only pulsar with a clear 2nd harmonic observed with *GINGA*. POWL \times double CYAB's cannot explain the spectrum. The continuum needs to fall off by itself (Nagase *et al.* 1991).

In order to solve those problems, it is a better and natural idea to assume that the continuum falls off thermally by itself. We tried some continuum models together with a single CYAB to the Her X-1 spectrum which has the best statistics. We started with the simplest $\exp(-E/kT) \times CYAB$, but failed. Next we tried Boltzmann model $E^\alpha \exp(-E/kT) \times CYAB$, which was successful in 13-60 keV. But α became positive ($\alpha = 0.74$) and cannot fit the negative POWL region below 10 keV. Then, by adding negative POWL, we introduce the NPEX (Negative and Positive power-laws

EXponential) model as

$$NPEx(E) = (A_1 E^{-\alpha_1} + A_2 E^{+\alpha_2}) \exp\left(-\frac{E}{kT}\right),$$

where kT is a typical temperature of the X-ray emitting plasma, and α_1 and α_2 are the negative and positive POWL indices, respectively.

The NPEX×CYAB model can fit the Her X-1 spectrum very well in the entire 2–60 keV energy band with an iron line included. Moreover the positive index converged to $\alpha_2 = 1.97 \pm 0.26$, which suggests the blackbody ($\alpha_2 = 2$). This model can fit the pulse-phase-resolved spectra, too.

Table 1: The best-fit parameters with NPEX×CYAB model for the pulse averaged spectra. Errors are in 90% confidence level. Positive POWL index α_2 is fixed to 2.0. The units of A_1 and A_2 are [photons/s/keV/4000cm²] at 10 keV. kT , E_a , W and E_{Fe} are in [keV], N_H is in [cm⁻²], and I_{Fe} is in [photons/s/4000cm²].

sources	Negative POWL		Pos. POWL	Exponential	Absorption
	A_1	α_1	A_2	kT	$\log_{10} N_H$
Her X-1	135 ± 8	0.51 ± 0.03	100 ± 23	8.0 ± 0.8	—
4U0115+63 (90)	491 ± 326	0.41 ± 0.48	4960 ± 1220	4.2 ± 0.1	—
4U0115+63 (91)	62 ± 22	0.65 ± 0.29	785 ± 58	4.3 ± 0.1	—
X0331+53	930 ± 63	-0.27 ± 0.05	630 ± 170	6.3 ± 0.5	—
1E2259+586	13 ± 12	1.42 ± 0.47	9 ± 7	2.1 fixed	—
LMC X-4	21 ± 1	0.43 ± 0.06	19 ± 2	7.3 ± 0.3	—
GS1843+00	45 ± 3	0.73 ± 0.08	47 ± 5	8.2 ± 0.2	22.29 ± 0.05
Cep X-4	101 ± 13	0.70 ± 0.05	110 ± 59	6.4 ± 1.5	22.01 ± 0.08
Vela X-1	171 ± 4	0.61 ± 0.05	123 ± 8	6.4 ± 0.1	22.41 ± 0.06
4U1907+09	11 ± 2	1.39 ± 0.29	25 ± 5	6.4 ± 0.7	22.86 ± 0.08
4U1538-52	19 ± 2	1.47 ± 0.20	68 ± 8	4.6 ± 0.2	22.80 ± 0.07
GX301-2	135 ± 71	0.80 ± 0.85	485 ± 184	5.4 ± 0.3	23.37 ± 0.07
	Leaky absorber, Norm $\times 0.38 \pm 0.26$				24.44 ± 0.22

sources		Resonance	Width	Depth	Iron Flux	Energy	χ^2_ν
		E_a	W	D	I_{Fe}	E_{Fe}	
Her X-1		33.1 ± 0.3	12.1 ± 1.7	1.53 ± 0.25	30 ± 4	6.65 fix	1.14
4U0115+63 (90)	1st	11.3 ± 0.6	5.9 ± 0.8	0.67 ± 0.08	17 ± 18	6.60 fix	0.69
	2nd	22.1 ± 0.4	5.2 ± 1.0	0.51 ± 0.07			
4U0115+63 (91)		15.6 ± 0.4	9.0 ± 0.6	1.22 ± 0.06	—	—	1.72
X0331+53		27.2 ± 0.3	7.5 ± 0.9	1.62 ± 0.15	38 ± 16	6.59 fix	1.65
1E2259+586		4.2 ± 0.6	2.0 ± 0.9	0.86 ± 0.27	—	—	8.71
LMC X-4		21.4 ± 1.2	5.1 ± 3.8	0.11 ± 0.05	2.7 ± 0.4	6.6 ± 0.1	0.83
GS1843+00		19.8 ± 2.1	9.9 ± 3.6	0.16 ± 0.05	7.6 ± 0.9	6.40 fix	0.49
Cep X-4		28.8 ± 0.4	12.1 ± 3.1	1.67 ± 0.59	7 ± 2	6.5 ± 0.1	0.97
Vela X-1	1st	24.5 ± 0.5	2.2 ± 1.0	0.065 ± 0.015	27 ± 3	6.5 ± 0.1	0.56
	2nd	$2E_{a1}$ fixed	$2W_1$ fixed	0.80 ± 0.26			
4U1907+09		18.9 ± 0.7	7.4 ± 2.1	0.87 ± 0.21	1.7 ± 0.5	6.60 fix	1.18
4U1538-52		20.6 ± 0.2	4.2 ± 0.6	0.83 ± 0.08	2.5 fixed	6.50 fix	1.58
GX301-2		37.6 ± 1.1	16.4 fixed	0.65 ± 0.17	32.1 ± 3.4	6.60 fix	0.98

We applied this model to other pulsars with α_2 fixed to 2. Only NPEX continuum is used to those without a cyclotron structure, NPEX×CYAB is used to those with a single structure, and NPEX×double CYAB's is used to those with two harmonics, which are 4U 0115+63 in 1990 and probably in Vela X-1. A merit of NPEX continuum model is that it is slightly concave as is often seen in the pulsar spectra in 2–10 keV range. With this continuum we discovered cyclotron structures from LMC X-4 and GS1843+00. The fitting parameters are summarized in Table 1.

MEANING OF NPEX MODEL

Let us consider the physical interpretation of the NPEX model. It would be natural to assume that kT is the typical temperature of the X-ray emitting plasma. We normalize the spectra with the energy of kT after correcting the detector efficiency and the absorption by the intervening matter. The flux level is normalized by the flux at $E = kT$ (Figure 1).

In the case of the non-cyclotron sources, the spectra obey a power law in the low energies, but with different indices, and show a round shoulder at around $E = 3kT$. Those are represented by the negative and positive POWL's of the NPEX model, respectively. As the slope of the power-law flattens, the hump at $E = 3kT$ increases, suggesting the existence of ONE hidden parameter which determines the shape of the continuum. The hidden parameter is also suggested from the pulse profiles sliced by some energy bands. Since the pulse shapes do not change below kT and above kT , the two POWL's cannot be independent, but are coupled by a hidden parameter.

In the case of the cyclotron sources, the overall curves are similar to those of the non-cyclotron sources. The difference is that the spectrum shows a steep fall-off at an energy, which is caused by the cyclotron resonance, and in some pulsars reaches a local minimum at the resonance center.

What mechanism creates both the negative POWL and the blackbody ? The multi-blackbody model would be possible, but an artificial distribution of temperature is needed. A better candidate is the Comptonization model. In fact the changes of the spectra in Figure 1 reminds us the Comptonized spectra for different optical depth τ . If a soft photon goes into the hot electron plasma, where scattering is more dominant than absorption, the photon gains energy by the inverse-Comptonization and comes out with a larger energy. When τ is small, the spectrum is a power law, and when τ is large, the Wien peak appears. τ can be the hidden parameter.

An analytic approximate calculation was done by Sunyaev and Titarchuk (1980) for a given soft photon input. The emergent photon spectrum is generally given as $(E^2 + o(E^2)) \exp(-E/kT)$, where $o(E^2)$ is the polynomials with lower order than 2. For example, when the input photon has an index of $\alpha = -2$ in the high energy wing, the output photon spectrum $F(x)$ is expressed as

$$F(x) \propto e^{-x} \left(\frac{x^2}{24} + \frac{x}{6} + \frac{1}{2} + \frac{1}{x} + \frac{1}{x^2} \right), \quad x \equiv E/(kT).$$

x^2 term corresponds to the positive POWL and the rest is combined to a negative POWL.

Figure 1 bottom is another Comptonization model by Lamb and Sanford (1979), (CMPL). It assumes a bremsstrahlung as the input photon. The change of the spectral shape with τ mimics that of the observed spectra. Thus, Comptonization model is a very possible candidate. The CMPL fits to the data ($\chi^2_\nu = 1 \sim 3$) are not as good as NPEX fits, but it represents the overall shapes well. It would be because the averaged spectrum cannot be represented by an ideal model.

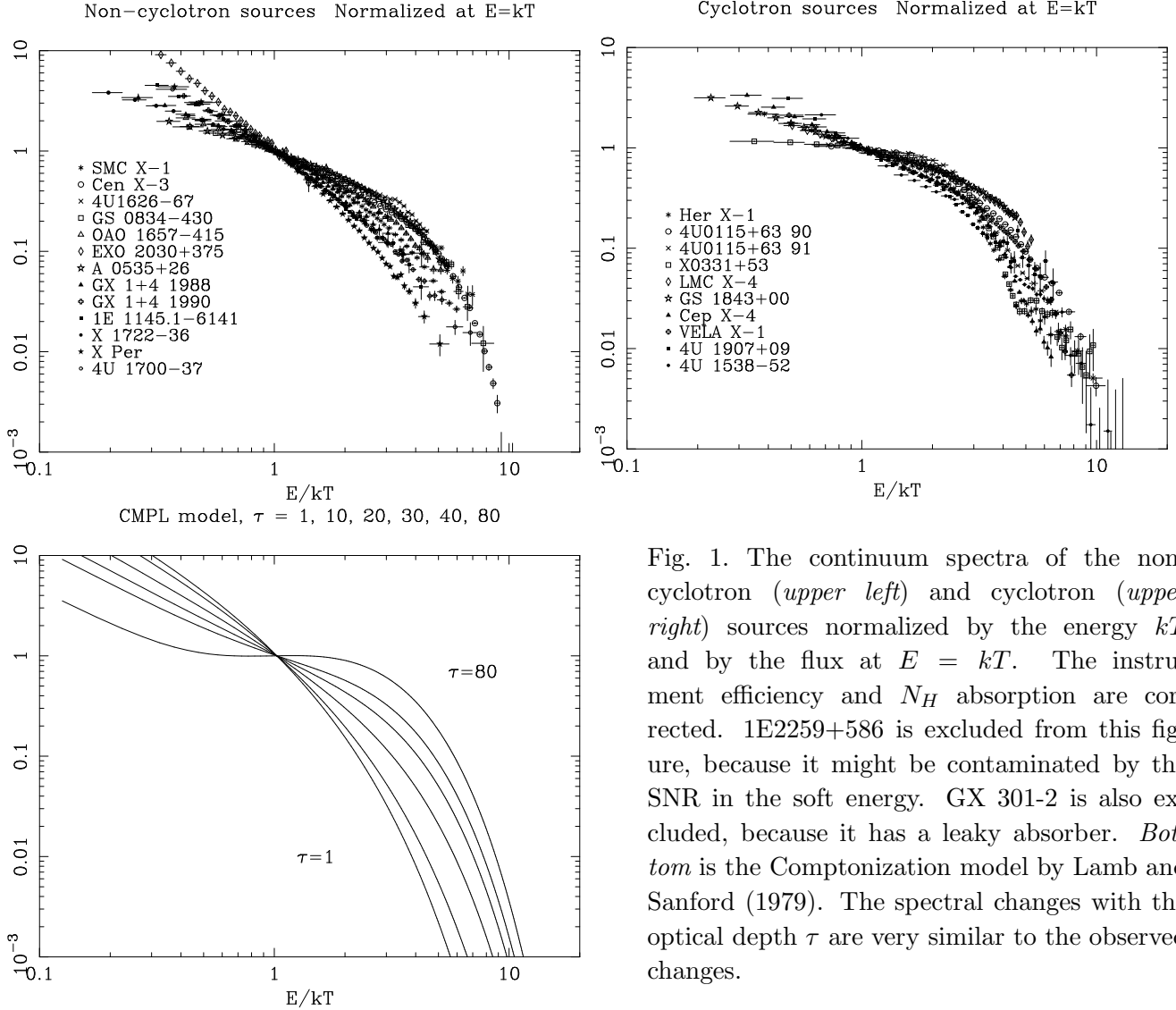


Fig. 1. The continuum spectra of the non-cyclotron (*upper left*) and cyclotron (*upper right*) sources normalized by the energy kT and by the flux at $E = kT$. The instrument efficiency and N_H absorption are corrected. 1E2259+586 is excluded from this figure, because it might be contaminated by the SNR in the soft energy. GX 301-2 is also excluded, because it has a leaky absorber. *Bottom* is the Comptonization model by Lamb and Sanford (1979). The spectral changes with the optical depth τ are very similar to the observed changes.

Then what determines those parameters? The obtained τ has a negative relation with kT . As τ becomes thick, kT goes down, while kT does not depend on L_X nor spin period. The only parameter which has a possible relation with kT is the resonance energy E_a (Figure 2). In the plasma where scattering is dominant, the energy transfer from an electron to a photon is given by the Kompaneets equation (eg. Rybicki and Lightman 1979), as $\Delta E = E/(mc^2)(4kT - E)$. In an equilibrium, $E = 4kT$. Now the interacting photons are mainly that with the resonance energy because the cross section is extremely large. Consequently the temperature of the electrons is ‘adjusted’ to satisfy equation $kT = 0.25E_a$. Monte-Carlo simulations of optically thick media by Lamb *et al.* (1990) find $kT \approx 0.27E_a$, and it is applied to the γ -ray bursts. The $kT = 0.25E_a$ relation, shown in Figure 2, is in a rough agreement with the data points.

Let us make sure that the Comptonization is the dominant process in the accretion column. Protons have most of the gravitational energy in the accreting matter. The time scales in which protons give energy to electrons, t_{col} , and electrons lose energy by the Comptonization, t_{comp} , are

$$t_{col} = 5 \times 10^{-5} n_{20}^{-1} \left(\frac{kT}{10 \text{ keV}} \right) [\text{s}], \quad t_{comp} = 1 \times 10^{-15} \left(\frac{kT}{10 \text{ keV}} \right)^{-4} [\text{s}]$$

(Gould 1982, Rybicki and Lightman 1979). Here n_{20} is the density in the unit of 10^{20} cm^{-3} , and Compton cross section is assumed to be $10^4 \sigma_T$ near the cyclotron resonance. Therefore electrons and photons interact much more strongly than protons and electrons, and electrons and photons are in the Comptonization equilibrium.

From the $E_a - kT$ relation one important suggestion can be deduced. Pulsars have kT between 4–14 keV (Table 1), which might indicate the cyclotron resonance energies are fairly constant within 10–60 keV. Moreover, the temperatures of the non-cyclotron sources are relatively higher than those of the cyclotron sources, which might mean that possible resonances are nearly at the high end of the energy range of *GINGA* and they are difficult to detected.

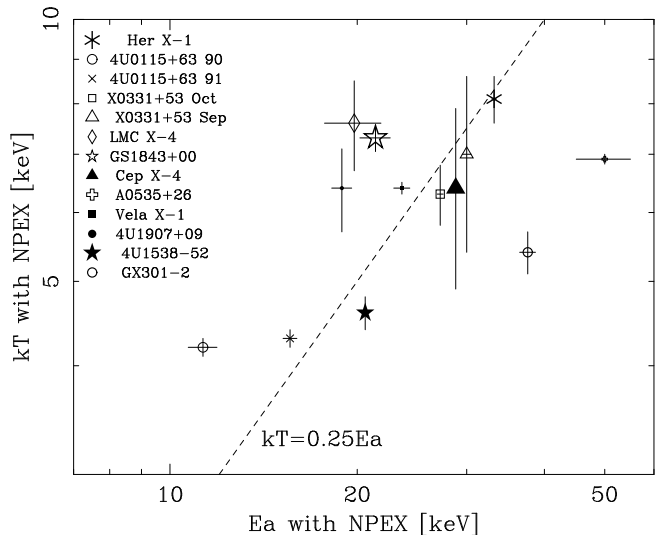


Fig. 2. Correlation between E_a and kT . There is a weak positive relation. If the Comptonization is dominant, $kT \approx 0.25E_a$ is expected.

What is the source of the input soft photons, then ? The bottom of the accretion column or the neutron star surface are candidates. From the observational view, Her X-1 has a strong soft 0.1keV blackbody component (McCray 1982). Although its origin is said to be the inner accretion disk or the Alfvén shell, some of it might come directly from the bottom of the accretion column.

We have used the Comptonization model without magnetic fields. Although the scattering cross section of an electron heavily depends on its energy in the magnetic fields, Meszaros (1992) notices that the continuum spectrum would be similar even in the magnetic fields except for the resonance. An absorption or an emission feature would be formed at around the resonance depending on the geometry and the optical depth of the scattering plasma. Readers might feel as if the Comptonized continuum is absorbed by CYAB, but it is not true. Those two are formed at the same time by the same scattering process.

MAGNETIC FIELDS DISTRIBUTION

We found the cyclotron structures from 11 pulsars among 23 X-ray pulsars including 1 pulsar-candidates. Adding A0535+26 from which *HEX*E discovered the cyclotron line (Kendziorra 1994), the cyclotron structures were detected from 12 pulsars, about a half of the 23 sources. Now we can make a distribution of the magnetic fields (Figure 3). The magnetic fields range between $3 \times 10^{11} - 5 \times 10^{12} \text{ G}$, which is similar to the life-corrected distribution of the radio pulsars (*right dotted line*), ranging between $10^{11} - 10^{13} \text{ G}$ with a peak at $2 \times 10^{12} \text{ G}$. The distribution of X-ray pulsars looks different from that of the *observed* radio pulsars (*right solid line*), which might indicate that the magnetic fields of the X-ray pulsars do not decay within a characteristic time scale of the radio pulsars ($10^6 - 10^7 \text{ y}$). As the magnetic fields of the radio pulsars are obtained assuming the magnetic dipole radiation, only the dipole component are measured. On the other hand, those measured by the X-ray cyclotron structure are almost on the surface of the neutron

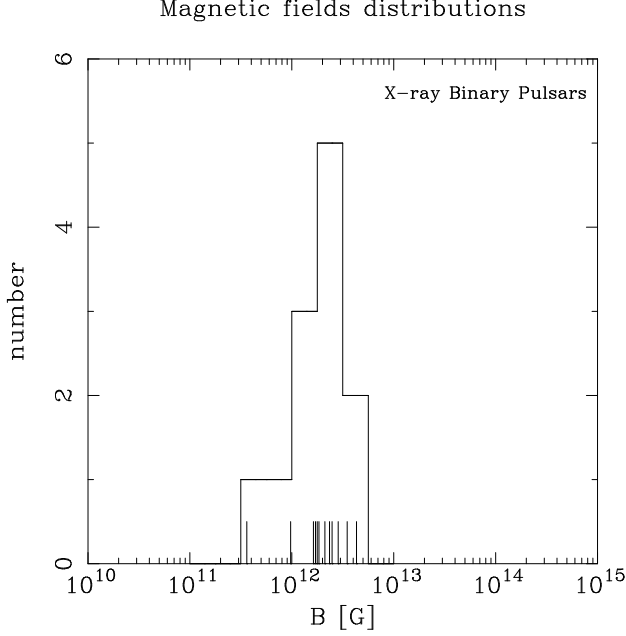


Fig. 3. The magnetic fields distribution of X-ray binary pulsars measured by the cyclotron resonances (*left*). The magnetic fields of the 12 pulsars are indicated with short lines on the horizontal axis. The distribution is similar to the life-corrected distribution of the radio pulsars (*right dotted line*), ranging in $10^{11} - 10^{13}$ G with a peak at 2×10^{12} G. The *right solid line* is that of the observed radio pulsars.

star and contain all multipole components. The agreement of the two indicates that the magnetic fields of the neutron star is dipole, and not multipole.

Let us discuss the selection effect. If there is a pulsar with a cyclotron resonance of less than a few keV, it is expected to show a steep power-law spectrum ($\alpha \sim 3$) in the *GINGA* energy range, as 1E2259+586. But all the other pulsars show a flat power-law in 2–10 keV, which suggests that pulsars with $E_a \lesssim 2$ keV does not exist. Although the detection limit towards the high energy is due to the *GINGA* energy range, kT and the $E_a - kT$ relation predict all the pulsars would have the cyclotron resonances in 4–60 keV. The pulsars with $E_a > 50$ keV are not likely. Since the data in Figure 3 already contain half the sources in the class, eventual inclusion of the others, even if all are at higher and lower energies, will not much change the distribution function of Figure 3. Thus, the magnetic field of X-ray binary pulsars are likely to cluster between $3 \times 10^{11} - 5 \times 10^{12}$ G.

RESONANCE ENERGY CHANGE

As shown in Figure 4 the cyclotron structure of 4U 0115+63 changed between the two observations. In 1990 it had double harmonic structures with the fundamental resonance at $E_a = 11$ keV. In 1991, however, it showed a broad single structure centered at $E_a = 16$ keV. It showed double/single structure throughout the pulse phases in 1990/1991, respectively. The luminosity in 1991 was 1/6 of that in 1990. *GINGA* observations of some sources with different intensities are summarized in Table 2. If we tentatively attribute the change of E_a to the height change of the scattering region ($E_a \propto r^{-3}$) and calculate the height difference assuming r in the weaker state is equal to the radius of the neutron star $R_{NS} = 10$ km, the height change is as much as 1.1 km in 4U 0115+63 as listed in Table 2 Δ height column.

Let us estimate the height of the accretion column employing the model by Burnard *et al.* (1991) to examine whether the change in height cited in Table 2 is reasonable or not. In the case of a pulsar, the accretion stream concentrates on the magnetic poles. Therefore Eddington limit of the emission along the magnetic fields is only $10^{35.7}$ erg/s. However, if the emission is sideward, most of the photon pressure is supported by the magnetic fields without stopping the accreting matter. Then the ‘Eddington limit’ L_1 becomes

$$L_1 = \theta_c L_{Edd} H_\perp \sim 10^{37.3} \frac{\theta_c}{0.1} \left(\frac{M_{NS}}{1.4 M_\odot} \right) H_\perp \text{ ergs/s.}$$

Here θ_c (~ 0.1) is the opening angle of the accretion column, H_\perp (~ 1.3) is the ratio of the Thomson cross section and the Rosseland averaged cross section for the radiation flow across B . L_{Edd} ($= 2.0 \times 10^{38}$ erg/s) is the conventional Eddington Luminosity by the Thomson scattering.

When a pulsar emits as much as L_1 , accretion flow yields a mound on the surface, whose height H_s would change in proportion to L_X .

$$H_s \approx \frac{L_X}{L_1} R_{NS} \theta_c = \frac{L_X}{L_{Edd} H_\perp} R_{NS} \quad (1)$$

Detailed calculations by Burnard *et al.* (1991) and Basko and Sunyaev (1976) justify this relation showing that the height H_s is the place where the radiation-dominated shock at Thomson optical depth $\sim 4 - 9$ transforms free fall matter into the subsonically settling on the mound.

We choose kT of the NPEX model as the temperature, assume $R_{NS} = 10$ km and $M_{NS} = 1.4 M_\odot$, and calculate H_\parallel and H_s as listed in Table 2. $E_a - H_s$ relations are shown in Figure 5. If we assume a dipole magnetic field ($B \propto r^{-3}$) and the gravitational redshift ($E_a \propto r^{0.34}$ in $r = 10 \sim 11$ km), the predicted H_s agree very well with the observations for X0331+53 and 4U 0115+63 as indicated by the dashed lines. The values of 4U 1538-52 are also consistent, since the low luminosity forms a low mound where the height change is negligibly small when the luminosity changes by 1.3. The measured magnetic field of 4U 1538-52 would be almost that on the surface of the neutron star. These very good agreements of the observations and predictions support the assumption that the change of the resonance energy is caused by the height change of the accretion column by the luminosity and that the magnetic field is dipole. Some questions, however, remain such as why the cyclotron scattering is dominated at the top of the accretion column while the most emission is from the bottom of it.

Her X-1 does not appear to obey the relation, and E_a is changing independently of L_X . However, it has the 35 d intensity cycle and there are many reasons to change the apparent luminosity of Her X-1, such as an increase of the scattering gas, occultation by the accretion disk, change of the X-ray beam and so on. The three points of E_a in 1989 were on one line, and a point in 1990 is off. The circumstances might not have changed much during the same or sequent main-on.

In Cep X-4 we cannot calculate H_s since we do not know the distance to it. But by assuming the relations (eq. 1) and $E_a \propto r^{-2.66}$, we can obtain the distance. Unknown parameters are the distance and the surface magnetic field and we have three data points to be fitted. We obtain the distance to Cep X-4 of 3.2 ± 0.4 kpc. The H_s are calculated to be 210 m, 170 m, and 110 m on 1988/4/3, 8, 14, respectively. The luminosities are $\log_{10} L_X = 36.75, 36.67$, and 36.48 , respectively. This can be a new method to estimate the distance to a binary X-ray pulsar.

NOTE: Cep X-4 was optically identified (Bonnet-Bidaud 1997, *IAU Circ.* 6724) using the position by ROSAT from the 1993 outburst (Schulz 1995, *A. & A.*, **295**, 413). The distance is 2.3-2.7 kpc from the reddening assuming the density of 1 H-atom cm^{-3} , or 3 kpc from the strong Na absorption line. Those are roughly consistent with our result.

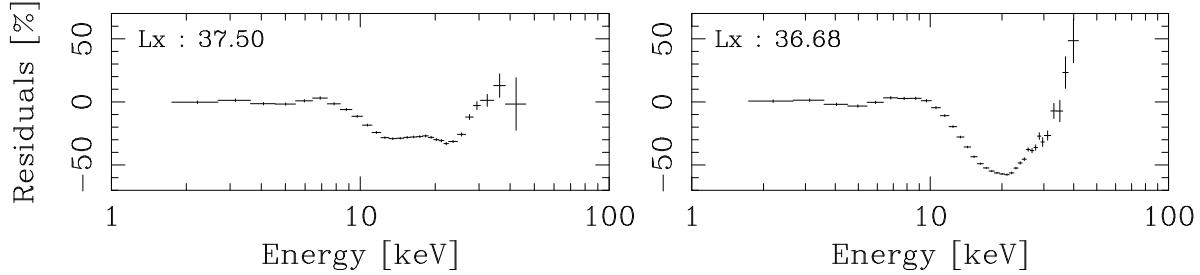


Fig. 4. Residuals from simple NPEX fits of 4U 0115+63 in 1990 (*left*) and 1991 (*right*). The cyclotron structure changed dramatically in the shape and the depth. The NPEX parameters are listed in Table 1.

REFERENCES

- Arons, J., R. I. Klein, and S. M. Lea, *Astrophys. J.*, **312**, 666 (1987).
 Basko, M. M., and R. A. Sunyaev, *Mon. Not. Roy. Astr. Soc.*, **175**, 395 (1976).
 Burnard, D. J., J. Arons, and R. I. Klein, *Astrophys. J.*, **367**, 575 (1991).
 Gould, R. J., Processes in Relativistic Plasmas, *Astrophys. J.*, **254**, 755 (1982).
 Kendziorra, E., P. Kretschmar, H. C. Pan, M. Kuntz, M. Maisack *et al.*, *A. & A.*, **291**, L31 (1994).
 Lamb, P. and P. W. Sanford, *Mon. Not. Roy. Astr. Soc.*, **188**, 555 (1979).
 Lamb, D. Q., C. L. Wang, and I. M. Wasserman, *Astrophys. J.*, **363**, 670 (1990).
 Makishima, K., and T. Mihara, Magnetic Fields of Neutron Stars, *Frontiers of X-ray Astronomy*, p23, ed. Y. Tanaka, and K. Koyama, Universal Academic Press Inc., Tokyo (1992).
 McCray, R. A., J. M. Shull, P. E. Boynton, J. E. Deeter, S. S. Holt, *et al.*, EINSTEIN Observatory Pulse-phase Spectroscopy of Hercules X-1, *Astrophys. J.*, **262**, 301 (1982).
 Meszaros, P., *High-Energy Radiation from Magnetized Neutron Stars*, University of Chicago Press (1992).
 Mihara, T., K. Makishima, T. Ohashi, T. Sakao, M. Tashiro *et al.*, *Nature*, **346**, 250 (1990).
 Mihara T., Ph.D. thesis for the physics degree of University of Tokyo (1995).
 Nagase, F., Accretion-Powered X-Ray Pulsars, *Publ. Astr. Soc. Japan*, **41**, 1 (1989).
 Nagase, F., T. Dotani, Y. Tanaka, K. Makishima, T. Mihara *et al.*, *Astrophys. J.*, **375**, L49 (1991).
 Rybicki, G. R. and Lightman, A. P., *Radiative Processes in Astrophysics*, John Wiley & Sons, Inc. (1979).
 Soong, Y., D. E. Gruber, L. E. Peterson, and R. E. Rothschild, *Astrophys. J.*, **348**, 641 (1990).
 Sunyaev, R. A. and Titarchuk, L. G., *A. & A.*, **86**, 121 (1980).
 Trümper, J., W. Pietsch, C. Reppin, W. Voges, R. Staubert *et al.*, *Astrophys. J.*, **219**, L105 (1978).
 Turner, M. J. L., H. D. Thomas, B. E. Patchett, D. H. Reading, K. Makishima *et al.*, The Large Area Counter on Ginga, *Publ. Astr. Soc. Japan*, **41**, 345 (1989).
 Wheaton, W. A., J. P. Doty, F. A. Primini, B. A. Cooke, C. A. Dobson *et al.*, *Nature*, **282**, 240 (1979).

Table 2: Cyclotron resonance energies with luminosities. H_{\parallel} is a function of E_a/kT and obtained from Arons *et al.* (1987). H_s is the height of the accretion column calculated by eq. (1) from L_X and H_{\parallel} assuming $M_{NS} = 1.4 M_{\odot}$, $R_{NS} = 10$ km, and $\theta_c = 0.1$.

sources	count rate	E_a	kT	$\log_{10} L_X$	Δheight	H_{\parallel}, H_{\perp}	H_s
date	[c/s]	[keV]	[keV]	[erg/s]	[m]		[m]
4U 0115+63	3–50 keV						
1990/2/11	4036	11.3 ± 0.6	4.25 ± 0.10	37.50	1100 ± 220	1.23	1280
1991/4/26	661	15.6 ± 0.4	4.34 ± 0.14	36.68	0		203
X0331+53	3–37 keV						
1989/10/1	3586	27.2 ± 0.3	6.3 ± 0.5	37.43	330 ± 70	1.44	930
1989/9/20	2271	30.0 ± 0.5	7.0 ± 1.6	37.29	0		674
Cep X-4	2–37 keV						
1988/4/3	834	28.58 ± 0.5 (± 0.05) ^a	7.5 ± 3.8	36.75^b	82 ± 109 (± 14)	1.38	210^b
1988/4/8	692	28.94 ± 0.4 (± 0.05) ^a	7.1 ± 2.2	36.67^b	40 ± 102 (± 14)		170^b
1988/4/14	450	29.29 ± 0.8 (± 0.11) ^a	6.4 ± 1.7	36.48^b	0		110^b
Her X-1	3–60 keV						
1990/7/27	1154	34.1 ± 0.4	8.1 ± 1.2	37.53	-160 ± 140	1.35	1250
1989/6/3	857	32.5 ± 1.0	10.3 ± 3.2	37.44	0 ± 110		1020
1989/6/6	792	32.5 ± 0.4	8.2 ± 0.9	37.40	0		930
1989/5/3	739	33.9 ± 1.2	9.7 ± 5.2	37.37	-140 ± 123		860
4U 1538-52	3–37 keV						
1988/3/2	184	20.6 ± 0.2	4.7 ± 0.3	36.56	0 ± 50	1.47	120
1990/7/27	130	20.6 ± 0.2	4.6 ± 0.2	36.43	0		91

a: Single parameter error, when other parameters than E_a are fixed to their best-fit values.

b: Estimated in this work assuming that the observed height changes are equal to the H_s changes. They would have very large errors because of the large errors of E_a . The most probable distance to Cep X-4 is 3.2 kpc.

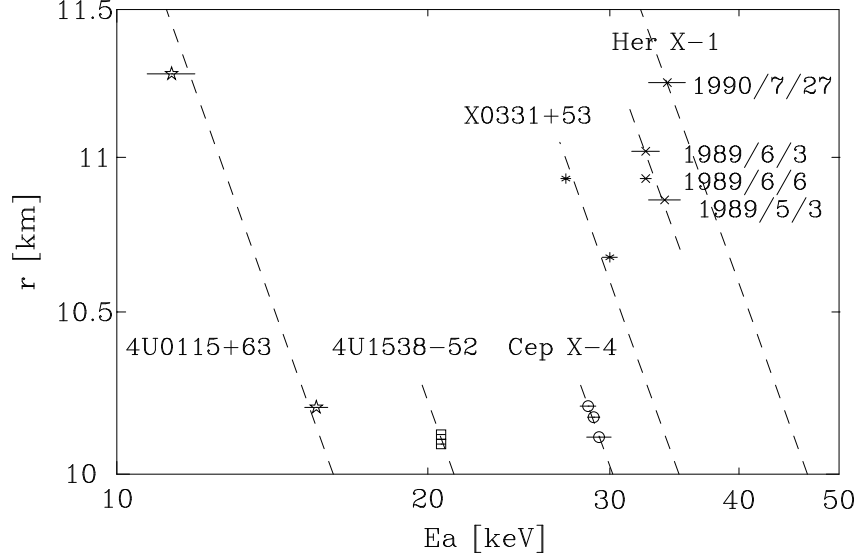


Fig. 5. The observed resonance energies and the heights of the accretion column estimated by a simple theory (eq. 1). r is the height from the center of the neutron star. $R_{NS} = 10$ km and $M_{NS} = 1.4M_{\odot}$ are assumed. The dashed line indicates $r^{-2.66}$ dependencies of the dipole magnetic field and the gravitational redshift. 4U0115+63, 4U1538-52, and X0331+53 obey this simple law well. Her X-1 does not obey this law, which would have other mechanisms to change the apparent luminosity. Assuming the $r^{-2.66}$ relation, the luminosities of Cep X-4 are calculated, which leads the distance to be 3.2 kpc.